

1 **Identifying SARS-CoV-2 entry inhibitors through drug repurposing screens of SARS- S**
2 **and MERS-S pseudotyped particles**

3

4 Catherine Z. Chen^{a#}, Miao Xu^{a#}, Manisha Pradhan^a, Kirill Gorshkov^a, Jennifer Petersen^b, Marco
5 R. Straus^c, Wei Zhu^a, Paul Shinn^a, Hui Guo^a, Min Shen^a, Carleen Klumpp-Thomas^a, Samuel G.
6 Michael^a, Joshua Zimmerberg^b, Wei Zheng^{a*}, Gary R. Whittaker^{c*}

7

8 ^aNational Center for Advancing Translational Sciences, National Institutes of Health, Rockville,
9 MD 20850

10 ^bSection on Integrative Biophysics, Division of Basic and Translational Biophysics, *Eunice*
11 *Kennedy Shriver* National Institute of Child Health and Human Development, National Institutes
12 of Health, Bethesda, MD 20892

13 ^cDepartment of Microbiology and Immunology, College of Veterinary Medicine, Cornell
14 University, Ithaca, NY 14853

15

16 [#]These authors contributed equally to this work

17

18 *To whom correspondence should be addressed:

19 Wei Zheng, Ph.D., wzheng@mail.nih.gov

20 Gary Whittaker, Ph.D., gary.whittaker@cornell.edu

21

22

23 **Running title:** SARS-S and MERS-S pseudotyped particle cell entry drug repurposing screens

1 **Identifying SARS-CoV-2 entry inhibitors through drug repurposing screens of SARS- S**
2 **and MERS-S pseudotyped particles**

3

4 **Abstract**

5 While vaccine development will hopefully quell the global pandemic of COVID-19 caused by
6 SARS-CoV-2, small molecule drugs that can effectively control SARS-CoV-2 infection are
7 urgently needed. Here inhibitors of two coronavirus spike proteins (S) were identified by
8 screening a library of approved drugs with SARS-S and MERS-S pseudotyped particle entry
9 assays. Using high-throughput screening technology, we discovered three compounds
10 (cepharanthine, abemaciclib and trimipramine) to be broad spectrum inhibitors for spike-
11 mediated entry. This work should contribute to the development of effective treatments against
12 the initial stage of viral infection, thus reducing viral burden in COVID-19 patients.

13

14 **Keywords:** SARS-CoV, MERS-CoV, SARS-CoV-2, drug repurposing screen, pseudotyped
15 particle viral entry assay

16

17

18

19

20

21

22

23

24

1 **Introduction**

2 Coronaviruses are enveloped, single-stranded, positive-sensed RNA viruses. While some
3 coronaviruses cause the common cold, others are highly pathogenic and have led to several
4 outbreaks in recent years [1]. In 2003, the coronavirus strain SARS-CoV caused severe acute
5 respiratory syndrome outbreak in Asia [2]. In 2013, the Middle East respiratory syndrome
6 (MERS) emerged with similar clinical symptoms as SARS, and the causative agent was named
7 MERS-CoV [3]. The coronavirus disease 2019 (COVID-19) was first identified in December
8 2019, and is caused by SARS-CoV-2, which was named based on sequence similarities to
9 SARS-CoV [4]. While many clinical trials are actively under way for treatment of COVID-19,
10 only remdesivir has gained emergency use authorization from the United States Food and Drug
11 Administration. However, it is already clear that this drug alone is not enough to combat the
12 COVID-19 pandemic [5]. Therefore, there is an unmet medical need to identify additional drugs
13 with anti-SARS-CoV-2 activity to ameliorate disease in hundreds of millions of yet infectible
14 individuals.

15 SARS-CoV-2 is a biological safety level 3 (BSL-3) pathogen. Currently, most facilities
16 for high-throughput screening (HTS) are only BSL-2, and few BSL-3 facilities have some HTS
17 capabilities. Several drug repurposing screens for SARS-CoV-2 have been reported, but the
18 throughput and assay type were limited due to biocontainment requirements. Therefore, the
19 development of BSL-2 compatible SARS-CoV-2 compound screening assays is an alternative
20 and more facile approach for HTS and drug development. Viral entry assays utilizing
21 pseudotyped particles (PP) are one type of cell-based BSL-2 viral assays that could be utilized
22 for this purpose. PP contain viral envelope proteins, but carry a reporter gene instead of the viral
23 genome, and thus display the necessary viral coat proteins for host receptor and membrane
24 interactions without the capacity for replication. These BSL-2 viral entry assays have been
25 successfully applied to HTS campaigns for several viruses such as Ebola virus [6], influenza [7],
26 and human immunodeficiency virus (HIV) [8].

27 For SARS-CoV and MERS-CoV, the spike proteins (S) are responsible for host receptor
28 binding and priming by host proteases to trigger membrane fusion. Thus, SARS-CoV and
29 MERS-CoV spike proteins were pseudotyped with murine leukemia virus (MLV) gag-pol
30 polyprotein to form SARS-S and MERS-S PP carrying luciferase reporter RNA [9,10]. The PP

1 entry assays include inoculation of susceptible cells with SARS-S or MERS-S PP, incubation to
2 allow luciferase reporter gene expression, and measurement of luciferase reporter activity. These
3 protocols were successfully optimized and miniaturized in 1536-well plate formats suitable for
4 HTS. Here, we report parallel drug repurposing screens using SARS-S and MERS-S PP entry
5 assays to identify a set of broad-spectrum coronavirus entry inhibitors. SARS-CoV-2 live virus
6 cytopathic effect (CPE) assay was used to test the generality of these coronavirus entry
7 inhibitors, confirming inhibition of SARS-CoV-2 entry.

8

9 **Materials and Methods**

10 *Reagents*

11 The following items were purchased from ThermoFisher: Dulbecco's Modified Eagle's
12 Medium (DMEM) (11965092), Pen/Strep (15140), TrypLE (12604013), PBS -/- (w/o Ca²⁺ or
13 Mg²⁺) (10010049), HCS Cell Mask Green (H32714), goat anti-mouse AlexaFluor 647
14 (A28175), and Hoechst 33342 (H3570). EMEM (30-2003) was purchased from ATCC. Hyclone
15 FBS (SH30071.03) was purchased from GE Healthcare. Pseudotyped particles (PP) for SARS-S
16 PP, MERS-S PP, VSV-G PP and delEnv PP (PP without fusion proteins) were produced by
17 Codex Biosolutions (Gaithersburg, MD) using previously reported methods [9,10]. Microplates
18 were purchased from Greiner Bio-One: white tissue-culture treated 96-well plates (655090),
19 black µclear 96-well plates (655083), white tissue-culture treated 384-well plates (781073), and
20 white tissue-culture treated 1536-well plates (789173-F). The following were purchased from
21 Promega: BrightGlo Luciferase Assay System (E2620), CellTiter-Glo Luminescent Cell
22 Viability Assay (G7573). ATPLite Luminescence Assay kit was purchased from PerkinElmer
23 (6016949). Cell Staining Buffer (420201) was purchased from BioLegend. Paraformaldehyde
24 (PFA) was purchased from Electron Microscopy Sciences (15714-S). Mouse-anti-firefly
25 luciferase antibody was purchased from Santa Cruz (sc-74548). SARS-S antibody was purchased
26 from BEI Resources (NR-617).

27

28 *Cell lines and cell culture*

1 Vero E6 cells (ATCC #CRL-1586) were cultured in EMEM with 10% FBS. Huh7 cells
2 (JCRB cell bank #JCRB0403) were cultured in DMEM with 10% FBS. Calu-3 cells (ATCC
3 #HTB-55) were cultured in EMEM with 10% FBS.

4

5 *Pseudotyped particle (PP) entry assays*

6 96-well format: Cells were seeded in 50 μ L/well media (20,000 cells/well for Vero E6
7 and Huh7, and 40,000 cells/well for Calu-3 cells), and incubated at 37°C, 5% CO₂ overnight
8 (~16 h). Supernatant was removed, and 50 μ L/well of PP was added. Plates were spin-inoculated
9 at 1500 rpm (453 xg) for 45 min, incubated for 2 h at 37°C, 5% CO₂, then 50 μ L/well of
10 growth media was added. The plates were incubated for 48 h at 37°C, 5% CO₂. The
11 supernatant was removed, 100 μ L/well of Bright-Glo (Promega) was added, incubated for 5 min
12 at room temperature, and luminescence signal was measured using a PHERAStar plate reader
13 (BMG Labtech).

14 384-well format: 10,000 cells/well of Calu-3 cells were seeded in 10 μ L media, and
15 incubated at 37°C, 5% CO₂ overnight (~16 h). Supernatant was removed, 10 μ L/well of 2x
16 compounds in media was added, incubated for 1 h, before 10 μ L/well PP was added. Plates were
17 spin-inoculated at 1500 rpm (453 xg) for 45 min, and incubated for 48 h at 37°C, 5% CO₂.
18 The supernatant was removed, 20 μ L/well of Bright-Glo (Promega) was added, incubated for 5
19 min at room temperature, and luminescence signal was measured using a PHERAStar plate
20 reader (BMG Labtech).

21 1536-well format: Cells were seeded at 2000 cells/well in 2 μ L media, and incubated at
22 37°C, 5% CO₂ overnight (~16 h). Compounds were titrated in DMSO, and 23 nL/well was
23 dispensed via an automated pintool workstation (Wako Automation). Plates were incubated for
24 1 h at 37C, 5% CO₂, and 2 μ L/well of PP was dispensed. Plates were spinoculated by
25 centrifugation at 1500 rpm (453 xg) for 45 min, and incubated for 48 h at 37°C, 5% CO₂.
26 After the incubation, the supernatant was removed with gentle centrifugation using a Blue
27 Washer (BlueCat Bio). Then, 4 μ L/well of Bright-Glo (Promega) was dispensed, incubated for 5
28 min at room temperature, and luminescence signal was measured using a ViewLux plate reader

1 (PerkinElmer). All data was normalized with wells containing PP as 100%, and delEnv PP as 0%
2 entry.

3

4 *ATP content cytotoxicity assay*

5 Cells were seeded at 1000 cells/well in 2 μ L/well media in 1536-well plates, and
6 incubated at 37°C, 5% CO₂ overnight (~16 h). Compounds were titrated in DMSO, 23 nL/well
7 was dispensed via an automated pintool workstation (Wako Automation). Plates were incubated
8 for 1 h at 37C, 5% CO₂, before 2 μ L/well of media was added. Plates were incubated for 48 h
9 at 37C, 5% CO₂. Then, 4 μ L/well of ATPLite (PerkinElmer) was dispensed, incubated for 15
10 min at room temperature, and luminescence signal was measured using a Viewlux plate reader
11 (PerkinElmer). Data was normalized with wells containing cells as 100%, and wells containing
12 media only as 0% viability.

13

14 *Drug repurposing screen and data analysis*

15 The NCATS pharmaceutical collection (NPC) was assembled internally, and contains
16 2,678 compounds, which include drugs approved by US FDA and foreign health agencies in
17 European Union, United Kingdom, Japan, Canada, and Australia, as well as some clinical trialed
18 experimental drugs [11]. The compounds were dissolved in 10 mM DMSO as stock solutions,
19 and titrated at 1:5 for primary screens with 4 concentrations, and at 1:3 for follow up assays with
20 11 concentrations. The SARS-S PP entry assay in Vero E6 cells, and MERS-S PP entry assay in
21 Huh7 cells, were used to screen the NPC library in parallel. Concurrently, counter screens for
22 cytotoxicity of compounds in Vero E6 and Huh7 were also screened against the NPC library.

23 A customized software developed in house at NCATS [12] was used for analyzing the
24 primary screen data. Half-maximal efficacious concentration (EC₅₀) and half-maximal
25 cytotoxicity concentration (CC₅₀) of compounds were calculated using Prism software
26 (GraphPad Software, San Diego, CA). Results in bar plots were expressed as mean of triplicates
27 \pm standard error of the mean (SEM).

28

1 *Luciferase immunofluorescence and high-content imaging*

2 Cells were seeded at 15,000 cells in 100 μ L/well media in 96-well assay plates, and
3 incubated at 37 \square °C, 5% CO₂ overnight (~16 h). Supernatant was removed, and 50 μ L/well of PP
4 was added. Plates were spin-inoculated at 1500 rpm (453 xg) for 45 min, incubated for 2 h at
5 37 \square °C, 5% CO₂, then 50 μ L/well of growth media was added. The plates were incubated for
6 48 \square h at 37 \square °C, 5% CO₂. Media was aspirated, and cells were washed once with 1X PBS
7 (ThermoFisher). Cells were then fixed in 4% PFA (EMS) in PBS containing 0.1% BSA
8 (ThermoFisher) for 30 min at room temperature. Plates were washed three times with 1X PBS,
9 then blocked and permeabilized with 0.1% Triton-X 100 (ThermoFisher) in Cell Staining Buffer
10 (Biolegend) for 30 min. Permeabilization/blocking solution was removed, 1:1000 primary
11 mouse-anti-luciferase antibody (Santa Cruz) was added, and incubated overnight at 4 °C.
12 Primary antibody was aspirated and cells were washed three times with 1X PBS. 1:1000
13 secondary antibody goat-anti-mouse-AlexaFluor 647 (ThermoFisher) was added for 1 h in Cell
14 Staining Buffer. Cells were washed three times, and stained with 1:5000 Hoechst 33342
15 (ThermoFisher) and 1:10000 HCS Cell Mask Green (ThermoFisher) for 30 min, before three
16 final 1X PBS washes. Plates were sealed and stored at 4 °C prior to imaging.

17 Plates were imaged on the IN Cell 2500 HS automated high-content imaging system. A
18 20x air objective was used to capture nine fields per well in each 96 well plate. Cells were
19 imaged with the DAPI, Green, and FarRed channels. Images were uploaded to the Columbus
20 Analyzer software for automated high-content analysis. Cells were first identified using the
21 Hoechst 33342 nuclear stain in the DAPI channel. Cell bodies were identified using the HCS
22 Cell Mask stain in the green channel using the initial population of Nuclei region of interests.
23 Intensity of the FarRed channel indicating luciferase expression was measured, and a threshold
24 was applied based on the background of the negative control. Average values, standard
25 deviations, and data counts were generated using pivot tables in Microsoft Excel and data was
26 plotted in Graphpad Prism.

27

28 *Negative stain and immunogold electron microscopy*

1 All reagents were obtained from Electron Microscopy Sciences, unless otherwise
2 specified. For negative staining without immunogold labeling, freshly glow-discharged, formvar
3 and carbon coated, 300-mesh copper grids were inverted on 5 μ l drops of sample on Parafilm for
4 1 min. Grids with adhered sample were transferred across two drops of syringe-filtered PBS, and
5 then two drops of filtered distilled water before being placed on a drop of 1% aqueous uranyl
6 acetate for 1 min, after which grids were blotted with filter paper, allowing a thin layer of uranyl
7 acetate to dry on the grid.

8 SARS-S PP to be immunogold labeled were adhered to freshly glow discharged, formvar
9 and carbon coated, 300-mesh gold grids, transferred across three drops of filtered PBS and then
10 incubated on drops of filtered blocking solution containing 2% BSA (Sigma) in PBS for 10 min.
11 Samples were covered during the incubation steps to prevent evaporation. Primary antibody to
12 SARS-S (BEI), was diluted 1:20 in filtered blocking solution. After blocking, grids were blotted
13 lightly with filter paper to remove excess solution before being transferred to primary antibody
14 droplets and incubated for 30 minutes. Then, grids were transferred across two drops of blocking
15 solution and incubated for 10 minutes. Secondary antibody (10 nm gold-conjugated Goat- α -
16 Mouse IgG) was diluted 1:20 in filtered blocking solution. Grids were lightly blotted before
17 transferred to droplets of secondary antibody, incubated for 30 min and then rinsed with 3 drops
18 of PBS. Prior to negative stain, grids were transferred across three drops of distilled water to
19 remove PBS as described above. Grids were observed using a ThermoFisher Tecnai T20
20 transmission electron microscope operated at 200 kV, and images were acquired using an AMT
21 NanoSprint1200 CMOS detector (Advanced Microscopy Techniques).

22

23 *SARS-CoV-2 cytopathic effect (CPE) assay*

24 SARS-CoV-2 CPE assay was conducted at Southern Research Institute (Birmingham,
25 AL). Briefly, compounds were titrated in DMSO and acoustically dispensed into 384-well assay
26 plates at 60 nL/well. Cell culture media (MEM, 1% Pen/Strep/GlutaMax, 1% HEPES, 2% HI
27 FBS) was dispensed at 5 μ L/well into assay plates and incubated at room temperature. Vero E6
28 (selected for high ACE2 expression) was inoculated with SARS CoV-2 (USA_WA1/2020) at
29 0.002 M.O.I. in media and quickly dispensed into assay plates as 4000 cells in 25 μ L/well. Assay
30 plates were incubated for 72 h at 37 \square °C, 5% CO₂, 90% humidity. Then, 30 μ L/well of CellTiter-

1 Glo (Promega) was dispensed, incubated for 10 min at room temperature, and luminescence
2 signal was read on an EnVision plate reader (PerkinElmer). An ATP content cytotoxicity assay
3 was conducted with the same protocol as CPE assay, without the addition of SARS-CoV-2 virus.

4

5 **Results**

6 *Optimization and miniaturization of SARS-S and MERS-S PP entry assays*

7 Both SARS-S and MERS-S PP were generated by a three plasmid co-transfection to yield
8 particles containing capsid protein of murine leukemia virus (MLV), spike protein (SARS-S or
9 MERS-S), and luciferase RNA (Figure 1a). The original entry assays were developed in 24-well
10 plates in which host cells were inoculated with PP. Upon cell entry, the particle releases the
11 luciferase RNA reporter for subsequent expression of the luciferase enzyme (Figure 1b) [9,10].
12 To optimize these assays for miniaturization into 1536-well plates, we first tested the SARS-S
13 and MERS-S PP entry in three cell lines: Vero E6, Huh7, and Calu-3. We found that Vero E6
14 cells produced the highest luciferase signal for SARS-S PP assay and that Huh7 cells yielded the
15 highest signal for MERS-S (Figure 2a). Vesicular stomatitis virus G glycoprotein (VSV-G) is a
16 class III fusion protein that constitutes the sole fusogenic protein, and does not require protease
17 priming [13]. Thus, VSV-G PP was used as a positive control and produced high signals for all
18 three cell lines (Figure 2a). This cell tropism data agrees with previous reports [10,14]. Based on
19 these results, the Vero E6 cell line and Huh7 cell line were chosen for SARS-S and MERS-S PP
20 entry assays, respectively. A time course experiment showed that higher signal-to-basal (S/B)
21 ratio was achieved with 48 h PP incubation with all glycoprotein-containing PP compared with
22 control PP formed by two plasmid transfection lacking envelope glycoproteins that are
23 responsible for membrane fusion (delEnv) (Figure 2b). Therefore, the 48 h time point was used
24 for all following experiments.

25 We examined the percentage of cells transduced with luciferase RNA by PP entry using
26 immunofluorescence staining of luciferase protein and found that in Vero E6 cells, SARS-S PP
27 and VSV-G PP produced 1.6% and 6.5% luciferase positive cells, respectively (Figure 2c). In
28 Huh7 cells, MERS-S PP and VSV-G pp transduction produced 10.9% and 26.8% luciferase
29 positive cells, respectively (Figure 2c). In all cells, the negative control delEnv PP and no PP

1 conditions produced negligible luciferase staining. The percentage of luciferase positive cells
2 correlated with luciferase enzyme activity when comparing different PP in the same cell line.
3 However, cell line comparisons did not show correlation between each PP, which may in part
4 reflect differences in the amount of luciferase expression per cell. The ultrastructure of SARS-S
5 and MERS-S PP were examined by negative stain electron microscopy (EM) to ensure that they
6 showed the expected morphology. EM analysis revealed regularly sized, 125-200 nm diameter
7 spherical structures, that were often partially or completely covered with a dense array of fine
8 filamentous or lollipop shaped projections, consistent with expected appearance of spike
9 glycoproteins (Figure 2d). The presence of SARS-S on the surface of SARS-S PP was further
10 confirmed by immunogold labeling (Figure 2d). MERS-S PP displayed a conspicuous dense coat
11 of spike-like structures, but lack of a primary antibody has thus far precluded confirmation of
12 their identity with immunogold labeling.

13 Both SARS-S and MERS-S PP entry assays were then miniaturized into 1536-well plate
14 format. The cell tropism pattern in the 1536-well format matched what was seen in the 96-well
15 format (Figure 2e). For SARS-S PP, the best assay performance was seen in Vero E6 cells
16 compared with delEnv PP, with S/B of 182.3, coefficient of variation (CV) of 24.1%, and a Z'
17 factor of 0.26. For MERS-S PP the best assay performance was seen in Huh7 cells, with an S/B
18 of 5325.8, CV of 10.9, and Z' factor of 0.67. Therefore, the SARS-S PP entry assay in Vero E6
19 cells, and MERS-S PP entry assay in Huh7 cells, were robust and advanced to HTS.

20

21 *SARS-S and MERS-S entry inhibitor drug repurposing screens*

22 The NCATS pharmaceutical collection (NPC) of 2,678 compounds that are either
23 approved or investigational drugs [11], was used for drug repurposing screens of both SARS-S
24 and MERS-S PP entry assays. The primary screens were carried out at four compound
25 concentrations (0.46, 2.3, 11.5, and 57.5 μ M). Compound cytotoxicity as determined by an ATP
26 content assay was counter screened in both Vero E6 and Huh7 cell lines, at the same
27 concentrations (Figure 3). All primary screening datasets were deposited to PubChem (Table 1).
28 The criteria to select hits for follow-up experiments include compounds in curve classes 1 and 2
29 with efficacy > 50% in the PP entry assay, and little to no cell killing effect in the cytotoxicity
30 assays using Vero E6 or Huh7 cells. Sixty-one and sixty-five compounds were identified as hits

1 from SARS-S and MERS-S PP viral entry assays, respectively. After removing 20 overlapping
2 hits, a total of 106 primary hits (4.0% hit rate) were selected for activity confirmation and
3 follow-up studies.

4

5 *Hit confirmation and follow up assays*

6 In our secondary assays, we retested the 106 cherry-picked hits in the same SARS-S and
7 MERS-S PP entry assays, along with ATP content cytotoxicity assays at 11 concentrations with
8 1:3 titration. PP entry assays rely on luciferase RNA reporter expression, a process which
9 involves the reverse transcription of luciferase RNA, integration into host genome, and
10 expression. Indeed, some of the confirmed hits had known mechanisms of action against reverse
11 transcriptase (adefovir and tenofovir disoproxil fumarate), and integrase (elvitegravir and
12 dolutegravir). Therefore, another counter assay, VSV-G PP entry assay, was tested in both Vero
13 E6 and Huh7 cell lines against the 106 hits. In addition to eliminating false positives that inhibit
14 luciferase expression, this assay identified compounds that specifically blocked spike
15 glycoprotein-mediated PP entry. All datasets for secondary assays are publicly available on
16 PubChem (Table 1).

17 These follow up assays yielded a set of 7 inhibitors that showed greater than 10-fold
18 selectivity to either SARS-S or MERS-S PP entry assays compared with the VSV-G PP entry
19 assays, and a safety index greater than 10 fold (CC_{50}/EC_{50}) (Figure 4a, b, Table 2). Of these 7
20 compounds, only cepharanthine was active against both SARS-S and MERS-S with greater than
21 10-fold selectivity. While trimipramine, copansilib, abemaciclib and osimertinib showed some
22 level of selectivity towards either SARS-S or MERS-S entry versus VSV-G entry, they only
23 reached 10-fold selectivity in one of the spike PP entry assays. Ingenol and NKH477 were only
24 active in SARS-S PP entry in Vero E6, and not in MERS-S entry in Huh7 cells.

25 These 7 confirmed entry inhibitors were then tested in SARS-S, MERS-S and VSV-G PP
26 entry assays in Calu-3 cells (Figure 4c). While most entry inhibitors failed to show selectivity
27 towards spike-mediated entry in Calu-3 cells, abemaciclib did show >10-fold selectivity towards
28 both SARS-S and MERS-S based entry compared with VSV-G.

29

1 *SARS-CoV-2 cytopathic effect assay to identify broad acting coronavirus entry inhibitors*

2 To test whether the confirmed SARS-S and MERS-S mediated PP entry inhibitors are
3 active against SARS-CoV-2, we further tested the top 8 compounds in a SARS-CoV-2
4 cytopathic effect (CPE) assay [15]. We found that 3 out of 8 entry inhibitors significantly
5 reduced (>30%) CPE caused by the SARS-CoV-2 infection in Vero E6 cells (Figure 5, Table 2).
6 Cephathine was found to be active against SARS-S in Vero E6 and MERS-S in Huh7 cells,
7 and inhibited SARS-CoV-2 CPE to near full efficacy with bell-shaped concentration response
8 due to cytotoxicity (Figure 5b). Trimipramine and abemaciclib also protected against SARS-
9 CoV-2 induced CPE to lesser degrees, with 48.1% and 41.7% CPE rescue, respectively (Figure
10 5a, e).

11

12 **Discussion**

13 Viruses rely on host cells for replication, and cell entry is the first step of the viral
14 infection life cycle, and a prime target for drug intervention. Both broad-spectrum and pathogen-
15 specific inhibitors of viral entry have been proposed for emerging viruses such as Ebola virus
16 and coronaviruses [16,17]. Proven therapeutics for viral entry include several approved drugs
17 targeting CCR5, the host co-receptor for HIV [18]. In SARS-CoV and SARS-CoV-2,
18 angiotensin-converting enzyme 2 (ACE2) has been recognized as a high affinity binding receptor
19 for the viral spike glycoprotein, while dipeptidyl peptidase-4 (DPP4) is the receptor for MERS-
20 CoV [19,20]. Following receptor binding, membrane fusion is mediated by spike protein
21 cleavage by host cell proteases. TMPRSS2 protease has been shown to be the predominant
22 protease in Calu-3 cells, which mediates ACE2-dependent direct membrane fusion that does not
23 involve the endocytic pathway [14]. Alternate entry pathways are used in cell lines such as Vero
24 E6 and Huh7 that involve endocytosis of viral particles and cathepsin protease priming for
25 membrane fusion [19]. Here, we have applied phenotypic SARS-S and MERS-S PP entry assays
26 for drug repurposing screens with the potential of identifying viral entry inhibitors with different
27 mechanisms of action.

28 In this study, we identified 7 coronavirus spike-driven entry inhibitors out of a library of
29 2,678 approved drugs (Figure 4). After further testing in a SARS-CoV-2 live virus CPE assay

1 and removing cytotoxic compounds, we identified three compounds (cepharanthine, abemaciclib,
2 and trimipramine) that rescued CPE of SARS-CoV-2 infection (Figure 5). Although the exact
3 mechanism for entry inhibition is unclear, these three compounds, inhibited SARS-S and MERS-
4 S PP cell entry with greater potency than VSV-G PP cell entry (Figure 4), indicating their
5 coronavirus-specific inhibitory activities on viral entry into host cells. Of these three,
6 cepharanthine and abemaciclib have been reported to rescue CPE of SARS-CoV-2 in Vero E6
7 cells [21]. Furthermore, in a recent report, cepharanthine was only able to block SARS-CoV-2
8 induced CPE in Vero E6 cells when added during the viral entry time period, but not during the
9 post-entry period, indicating that its anti-SARS-CoV-2 activity is through entry inhibition [22].
10 Cepharanthine is a natural product used in Japan since the 1950s for treatments of several
11 diseases without major side effects [23]. It has polypharmacology, with anti-inflammatory
12 activity linked to AMPK activation and NF κ B inhibition [23]. Cepharanthine has previously
13 reported antiviral activities against HIV, SARS-CoV, HCoV-OC43, human T-lymphotropic virus
14 (HTLV) and hepatitis B virus (HBV) [24].

15 Abemaciclib was another drug that exhibited selective inhibition of the SARS-CoV PP
16 and MERS-CoV PP entry compared to control VSV-G PP, and rescued SARS-CoV-2 CPE
17 (Figure 4 and 5). Abemaciclib is a CDK4/6 inhibitor that has been in clinical trials for treatment
18 of breast cancer [25,26]. Cyclin-dependent kinases (CDK) are a group of serine-threonine
19 kinases that regulate the cell cycle, and have been targeted for anticancer drug development.
20 Additionally, antiviral activities of CDK inhibitors have been reported against HIV, herpes
21 simplex virus (HSV), HBV and Zika virus [27]. The antiviral mechanism of action for CDK
22 inhibitors works mainly through the suppression of viral genome replication in host cells [27].
23 Our data suggests that abemaciclib inhibits CPE of SARS-CoV-2 by blocking cell entry in Vero
24 E6, Huh7 and Calu-3 cells. Therefore, the structure of this compound may have the potential to
25 be optimized as a more potent SARS-CoV-2 entry inhibitor.

26 Trimipramine is an oral tricyclic antidepressant. Chemically, trimipramine is a basic
27 amine compound belonging to cationic amphiphilic drugs. The antiviral activity of trimipramine
28 has been reported to block the viral entry for Ebola virus and influenza [28,29]. Due to its
29 chemical property, trimipramine as a basic amine can accumulate in acidic organelles such as the
30 late endosomes and lysosomes in cells. High concentration of basic amine drugs in late

1 endosomes and lysosomes may block viral genome release into cytosol [28,29]. However, for
2 coronaviruses, this effect might be more prominent in cell lines such as Vero E6 and Huh7, but
3 not in Calu-3 cells, which has endocytosis independent entry [19]. In accordance with this,
4 trimipramine's entry inhibition activity was not confirmed in Calu-3 cells (Figure 4).
5 Importantly, the antiviral entry activity of trimipramine has not yet been reported. In addition,
6 clomipramine, a close analog of trimipramine, was also reported to protect against SARS-CoV-2
7 CPE through inhibition of autophagy [15]. In the current study, clomipramine was found to be
8 active against SARS-S PP entry and non-cytotoxic in the primary screen, but was not selected for
9 further follow-up because its potency was below the threshold criteria.

10 A number of drug repurposing and computer-aided virtual screens have been reported for
11 SARS-CoV-2. It is a common phenomenon that the potencies identified in drug repurposing are
12 not high enough to be clinically relevant when compared to the human plasma concentrations
13 achievable at approved dosing regimens [30]. Drug combination therapy has been proposed as a
14 practical and useful approach for drug repurposing to treat emerging infectious diseases, as drug
15 synergy may reduce the individual drug concentrations in the combinations. The synergistic
16 effect of two- or three- drug combination therapy can increase the therapeutic effect, reduce the
17 doses of individual drugs, and thus reduce potential adverse effects [30]. Ohashi H et al. has
18 reported that the combination of cepharanthine (entry inhibitor) and nelfinavir (HIV protease
19 inhibitor) enhanced the anti-SARS-CoV-2 activity [22]. We believe that these coronavirus
20 specific viral entry inhibitors may have utility in a drug combination therapy with other anti-
21 SARS-CoV-2 drugs that have different mechanisms of action, such as remdesivir (the viral RNA
22 dependent RNA polymerase inhibitor), or lysomotropic autophagy inhibitors.

23

24

25

26 **Ethics Statement**

27 The authors declared no potential conflicts of interest with respect to the research, authorship,
28 and/or publication of this article.

1

2 **Author Contributions**

3 MX, MP, KG, WZhu, MS and JP performed experiments; CZC and WZheng made the
4 conceptualization and data curation; MS and GH analyzed data; CZC and WZheng wrote the
5 manuscript, and all authors edited the manuscript.

6

7 **Acknowledgement**

8 This work is funded by the Intramural Research Program of the National Center for Advancing
9 Translational Sciences, and National Institute of Child Health and Human Development,
10 National Institutes of Health. Work in the author's laboratory (GW) is supported by the National
11 Institutes of Health (research grant R01AI35270).

1 References

- 2 1. Mandell GL, Bennett JE, Dolin R. Mandell, Douglas, and Bennett's principles and practice of
3 infectious diseases. 7th ed. Philadelphia, PA: Churchill Livingstone/Elsevier; 2010.
- 4 2. Drosten C, Gunther S, Preiser W, et al. Identification of a novel coronavirus in patients with
5 severe acute respiratory syndrome. *N Engl J Med*. 2003 May 15;348(20):1967-76.
- 6 3. Zaki AM, van Boheemen S, Bestebroer TM, et al. Isolation of a novel coronavirus from a man
7 with pneumonia in Saudi Arabia. *N Engl J Med*. 2012 Nov 8;367(19):1814-20.
- 8 4. Lu R, Zhao X, Li J, et al. Genomic characterisation and epidemiology of 2019 novel coronavirus:
9 implications for virus origins and receptor binding. *Lancet*. 2020 Feb 22;395(10224):565-574.
- 10 5. Beigel JH, Tomashek KM, Dodd LE, et al. Remdesivir for the Treatment of Covid-19 - Preliminary
11 Report. *N Engl J Med*. 2020 May 22.
- 12 6. Kouznetsova J, Sun W, Martinez-Romero C, et al. Identification of 53 compounds that block
13 Ebola virus-like particle entry via a repurposing screen of approved drugs. *Emerg Microbes
14 Infect*. 2014 Dec;3(12):e84.
- 15 7. Weisshaar M, Cox R, Morehouse Z, et al. Identification and Characterization of Influenza Virus
16 Entry Inhibitors through Dual Myxovirus High-Throughput Screening. *J Virol*. 2016 Aug
17 15;90(16):7368-7387.
- 18 8. Garcia JM, Gao A, He PL, et al. High-throughput screening using pseudotyped lentiviral particles:
19 a strategy for the identification of HIV-1 inhibitors in a cell-based assay. *Antiviral Res*. 2009
20 Mar;81(3):239-47.
- 21 9. Millet JK, Tang T, Nathan L, et al. Production of Pseudotyped Particles to Study Highly
22 Pathogenic Coronaviruses in a Biosafety Level 2 Setting. *J Vis Exp*. 2019 Mar 1(145).
- 23 10. Millet JK, Whittaker GR. Murine Leukemia Virus (MLV)-based Coronavirus Spike-pseudotyped
24 Particle Production and Infection. *Bio Protoc*. 2016 Dec 5;6(23).
- 25 11. Huang R, Zhu H, Shinn P, et al. The NCATS Pharmaceutical Collection: a 10-year update. *Drug
26 Discov Today*. 2019 Dec;24(12):2341-2349.
- 27 12. Wang Y, Jadhav A, Southal N, et al. A grid algorithm for high throughput fitting of dose-response
28 curve data. *Curr Chem Genomics*. 2010 Oct 21;4:57-66.
- 29 13. Kim IS, Jenni S, Stanifer ML, et al. Mechanism of membrane fusion induced by vesicular
30 stomatitis virus G protein. *Proc Natl Acad Sci U S A*. 2017 Jan 3;114(1):E28-E36.
- 31 14. Hoffmann M, Kleine-Weber H, Schroeder S, et al. SARS-CoV-2 Cell Entry Depends on ACE2 and
32 TMPRSS2 and Is Blocked by a Clinically Proven Protease Inhibitor. *Cell*. 2020 Apr 16;181(2):271-
33 280 e8.
- 34 15. Gorshkov K, Chen CZ, Bostwick R, et al. The SARS-CoV-2 cytopathic effect is blocked with
35 autophagy modulators. *bioRxiv*. 2020 May 28.
- 36 16. Xia S, Liu M, Wang C, et al. Inhibition of SARS-CoV-2 (previously 2019-nCoV) infection by a highly
37 potent pan-coronavirus fusion inhibitor targeting its spike protein that harbors a high capacity to
38 mediate membrane fusion. *Cell Res*. 2020 Apr;30(4):343-355.
- 39 17. Zhou Y, Simmons G. Development of novel entry inhibitors targeting emerging viruses. *Expert
40 Rev Anti Infect Ther*. 2012 Oct;10(10):1129-38.
- 41 18. Arts EJ, Hazuda DJ. HIV-1 antiretroviral drug therapy. *Cold Spring Harb Perspect Med*. 2012
42 Apr;2(4):a007161.
- 43 19. Tang T, Bidon M, Jaimes JA, et al. Coronavirus membrane fusion mechanism offers a potential
44 target for antiviral development. *Antiviral Res*. 2020 Apr 6;178:104792.
- 45 20. Wrapp D, Wang N, Corbett KS, et al. Cryo-EM structure of the 2019-nCoV spike in the prefusion
46 conformation. *Science*. 2020 Mar 13;367(6483):1260-1263.

- 1 21. Jeon S, Ko M, Lee J, et al. Identification of Antiviral Drug Candidates against SARS-CoV-2 from
2 FDA-Approved Drugs. *Antimicrob Agents Chemother*. 2020 Jun 23;64(7).
- 3 22. Ohashi H, Watashi K, Saso W, et al. Multidrug treatment with nelfinavir and cepharanthine
4 against COVID-19. *bioRxiv*. 2020 April 15.
- 5 23. Bailly C. Cepharanthine: An update of its mode of action, pharmacological properties and
6 medical applications. *Phytomedicine*. 2019 Sep;62:152956.
- 7 24. Rogosnitzky M, Okediji P, Koman I. Cepharanthine: A review of the antiviral potential of a
8 Japanese-approved alopecia drug in COVID-19. *OSF Preprints*. 2020 May 13.
- 9 25. Eggersmann TK, Degenhardt T, Gluz O, et al. CDK4/6 Inhibitors Expand the Therapeutic Options
10 in Breast Cancer: Palbociclib, Ribociclib and Abemaciclib. *BioDrugs*. 2019 Apr;33(2):125-135.
- 11 26. Poratti M, Marzaro G. Third-generation CDK inhibitors: A review on the synthesis and binding
12 modes of Palbociclib, Ribociclib and Abemaciclib. *Eur J Med Chem*. 2019 Jun 15;172:143-153.
- 13 27. Schang LM, St Vincent MR, Lacasse JJ. Five years of progress on cyclin-dependent kinases and
14 other cellular proteins as potential targets for antiviral drugs. *Antivir Chem Chemother*.
15 2006;17(6):293-320.
- 16 28. Salata C, Calistri A, Alvisi G, et al. Ebola Virus Entry: From Molecular Characterization to Drug
17 Discovery. *Viruses*. 2019 Mar 19;11(3).
- 18 29. Salata C, Calistri A, Parolin C, et al. Antiviral activity of cationic amphiphilic drugs. *Expert Rev Anti*
19 *Infect Ther*. 2017 May;15(5):483-492.
- 20 30. Zheng W, Sun W, Simeonov A. Drug repurposing screens and synergistic drug-combinations for
21 infectious diseases. *Br J Pharmacol*. 2018 Jan;175(2):181-191.

22

- 1 **Table 1.** PubChem assay IDs (AIDs). Datasets can be found at
- 2 <https://pubchem.ncbi.nlm.nih.gov/> under the following AIDs.

AID	# of Compounds	Concentration response format	Assay	Cell line
1479145	2678	4-pt, 1:5	SARS-S PP entry	Vero E6
1479150	2678	4-pt, 1:5	Cytotoxicity	Vero E6
1479149	2678	4-pt, 1:5	MERS-S PP entry	Huh7
1479147	2678	4-pt, 1:5	Cytotoxicity	Huh7
1479148	106	11-pt, 1:3	SARS-S PP entry	Vero E6
1494158	106	11-pt, 1:3	VSV-G PP entry	Vero E6
1479144	106	11-pt, 1:3	Cytotoxicity	Vero E6
1494157	106	11-pt, 1:3	MERS-S PP entry	Huh7
1494156	106	11-pt, 1:3	VSV-G PP entry	Huh7
1479146	106	11-pt, 1:3	Cytotoxicity	Huh7

3

4

5

1 **Table 2.** SARS-S and MERS-S selective compounds and their anti-SARS-CoV-2 activity

2 N/A = Not active, highest concentration tested is listed.

3 MOA = Mechanism of action

<u>Compound Name</u> (MOA)	SARS-S PP in Vero E6		VSV-G PP in Vero E6		Vero E6 Cytotoxicity		SARS-CoV-2 CPE		SARS-CoV-2 Cytotoxicity	
	EC50 (μM)	Efficacy (%)	EC50 (μM)	Efficacy (%)	CC50 (μM)	Efficacy (%)	EC50 (μM)	Efficacy (%)	CC50 (μM)	Efficacy (%)
<u>Ethaverine</u> (Smooth muscle relaxant)	0.07	63.5	8.57	106.3	27.10	69.8	N/A, >20	0.0	N/A, >20	0.0
<u>NKH477</u> (Adenylyl cyclase activator)	1.36	71.4	N/A, >57.5	0.0	N/A, >57.5	0.0	N/A, >20	28.6	7.08	57.3
<u>Trimipramine</u> (Tricyclic antidepressant)	4.29	90.9	30.40	29.2	54.06	16.6	10	48.4	N/A, >20	0.0
<u>Osimertinib</u> (EGFR inhibitor)	2.71	117.5	42.94	118.4	17.10	99.6	N/A, >20	29.0	11.22	117.9
<u>Ingenol</u> (Topical anti-tumor medication)	0.02	93.3	0.24	76.4	0.00	-4.0	N/A, >20	0.0	N/A, >20	0.0
<u>Cepharanthine</u> (Antiinflammatory, antineoplastic)	1.92	90.9	21.52	76.9	42.94	106.2	2.00	92.5	N/A, >20	0.0
<u>Compound Name</u> (MOA)	MERS-S PP in Huh7		VSV-G PP in Huh7		Huh7 Cytotoxicity					
	EC50 (uM)	Efficacy (%)	EC50 (uM)	Efficacy (%)	CC50 (uM)	Efficacy (%)				
<u>Abemaciclib</u> (CDK inhibitor)	0.38	82.3	0.27	27.1	17.10	90.0	7.94	41.7	11.22	72.2
<u>Copanlisib</u> (PI3K inhibitor)	3.12	65.8	9.87	6.2	1.75	13.6	N/A, >20	0.0	0.14	45.3
<u>Cepharanthine</u> (Antiinflammatory, antineoplastic)	1.71	108.4	24.15	115.3	38.27	88.9	2.00	92.5	N/A, >20	0.0

4

5

1 **Figure Captions**

2

3 **Figure 1.** Illustration of pseudotyped particle generation and entry assay. (a) Three plasmids
4 (pCMV-MLVgag-pol, pcDNA-SARS-S/MERS-S, and pTG-Luc) are co-transfected into HEK-
5 293T/17 cells. The plasmids express MLV core gag-pol polyprotein, coronavirus spike
6 glycoproteins, and luciferase RNAs, which together assemble into pseudotyped particles. (b)
7 Comparison of SARS/MERS-CoV and pseudotyped particle, showing shared spike proteins to
8 facilitate entry into target cell. Once cell entry occurs, RNAs of pseudotyped particles are
9 released into cell, where they are reverse transcribed into DNAs, integrated into the genome, and
10 express luciferase reporter enzyme. Illustrations were made with BioRender.

11

12 **Figure 2.** Assay optimization. (a) Entry of SARS-S, MERS-S, delEnv and VSV-G pseudotyped
13 particles (PP) in Vero E6, Huh7 and Calu-3 cells as assayed by luciferase reporter expression.
14 RLU = relative luminescence units. (b) Cell entry time course of PP. Luciferase reporter activity
15 is assayed at 24 h and 48 h after PP addition. (c) Representative image montage of Vero E6 and
16 Huh7 cells treated with VSV-G, SARS-S, or delEnv PP for 72 hours and immunostained using
17 mouse-anti-luciferase antibody (magenta). Cells were also stained with Hoechst 33342 (cyan) for
18 nuclei and HCS Cell Mask Green (yellow) for cell bodies. Images were captured using a 20x
19 objective. Graphs on the right panel are high-content imaging measurements of the percentage of
20 cells that are positive for luciferase expression. Positive cells were identified using a cell
21 intensity threshold and the number of transfected cells was divided by the total cell count in the
22 field. N = 9 fields per well in three wells. Error bars indicate S.D. (d) PP ultrastructure was
23 examined by negative stain EM. Individual PP decorated with spike-like projections were
24 observed. The presence of spike glycoproteins on the surface of SARS-S PP was confirmed by
25 10 nm-immunogold labeling (black dots). MERS PP displayed a dense array of spike-like
26 projections. Scale bar = 100 nm. (e) PP entry assay was miniaturized to 1536-well format and
27 performance of SARS-S, MERS-S, delEnv and VSV-G PP in Vero E6, Huh7 and Calu-3 cells
28 are shown.

29

1 **Figure 3.** Schematic of repurposing screen and follow up assays.

2

3 **Figure 4.** Concentration response of entry inhibitors. (a) Concentration response of entry
4 inhibitors against SARS-S and VSV-G PP entry in Vero E6 cells. (b) Concentration response of
5 entry inhibitors against MERS-S and VSV-G PP entry in Huh7 cells. (c) Concentration response
6 of entry inhibitors against SARS-S, MERS-S and VSV-G PP entry in Calu-3 cells. (d)
7 Compound structures.

8

9 **Figure 5.** SARS-CoV-2 CPE assay and cytotoxicity concentration response for (a)
10 Trimipramine, (b) Cepharanthine, (c) Ingenol, (d) Copanisib, (e) Abemaciclib, (f) Osimertinib,
11 and (g) NKH477.

Figure 1.

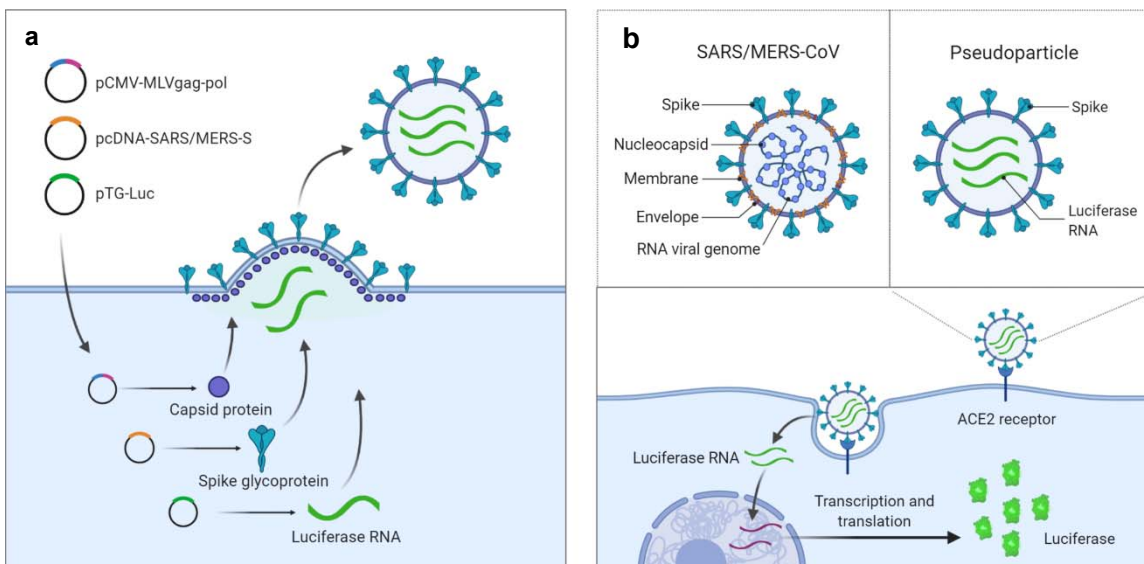
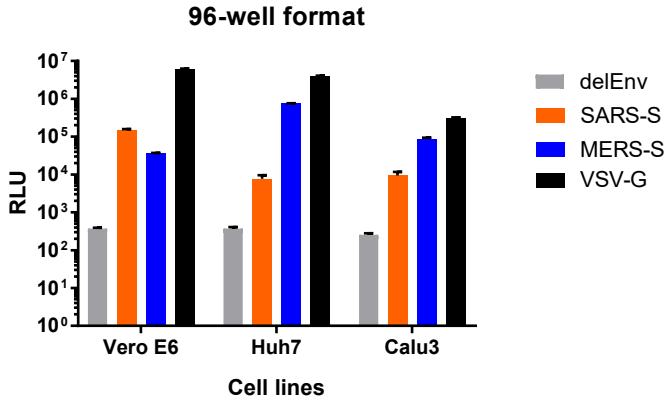
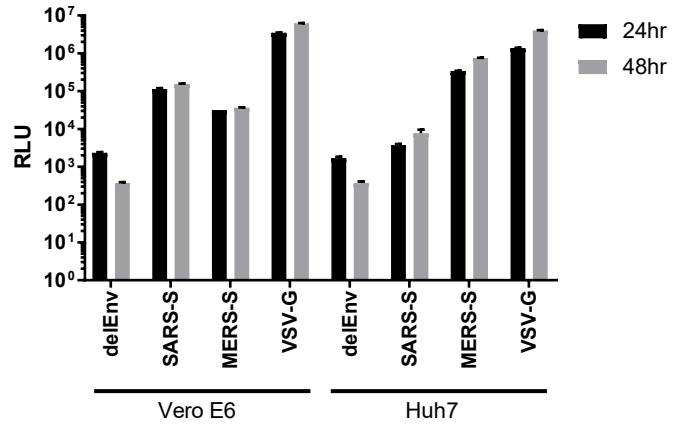


Figure 2.

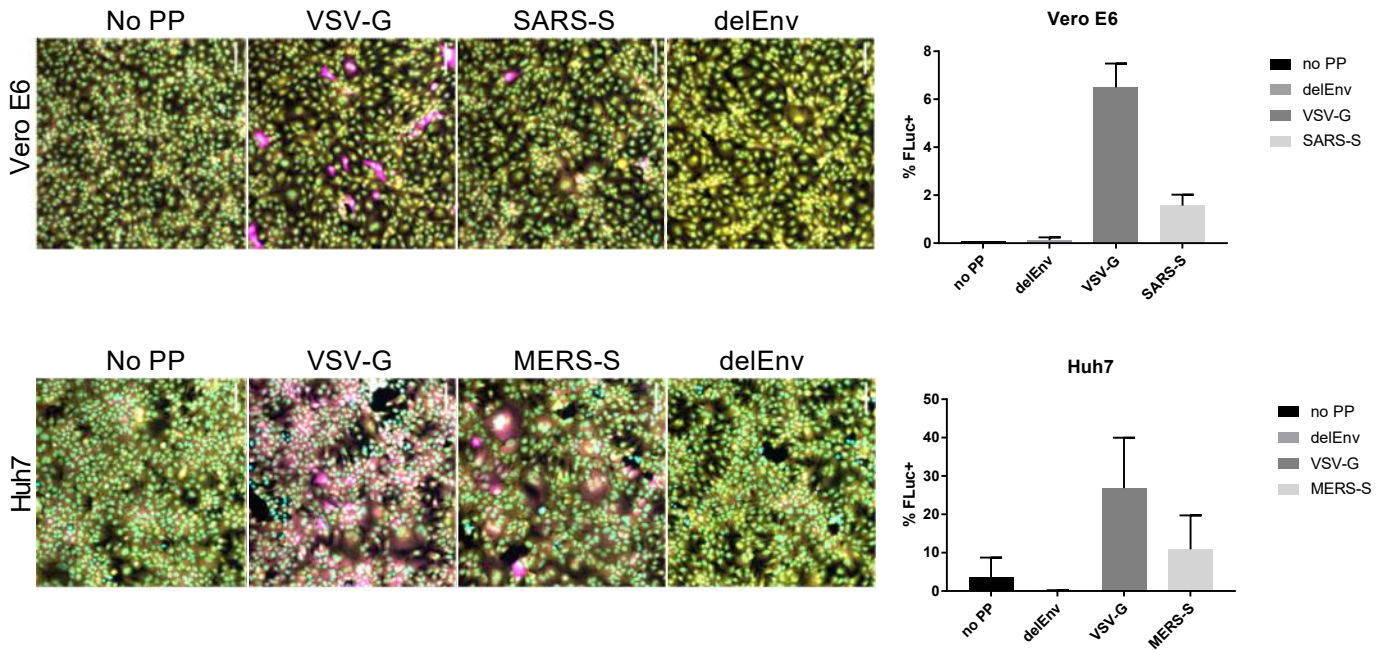
a. Cell line screen



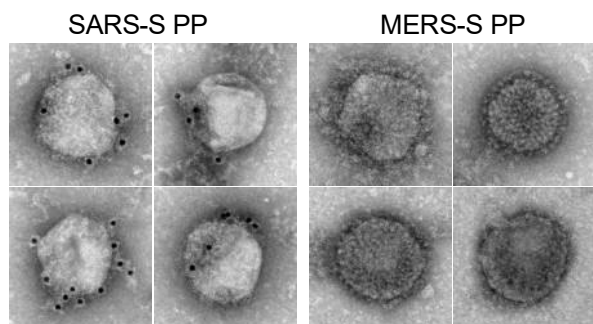
b. Time course



c. Percent luciferase transduction



d. Pseudotyped particle ultrastructure



e. Assay miniaturization

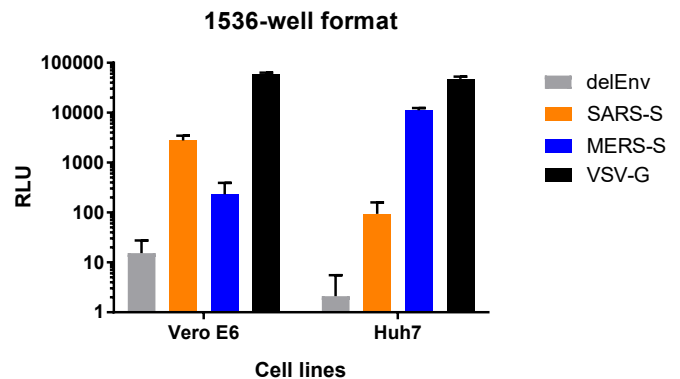
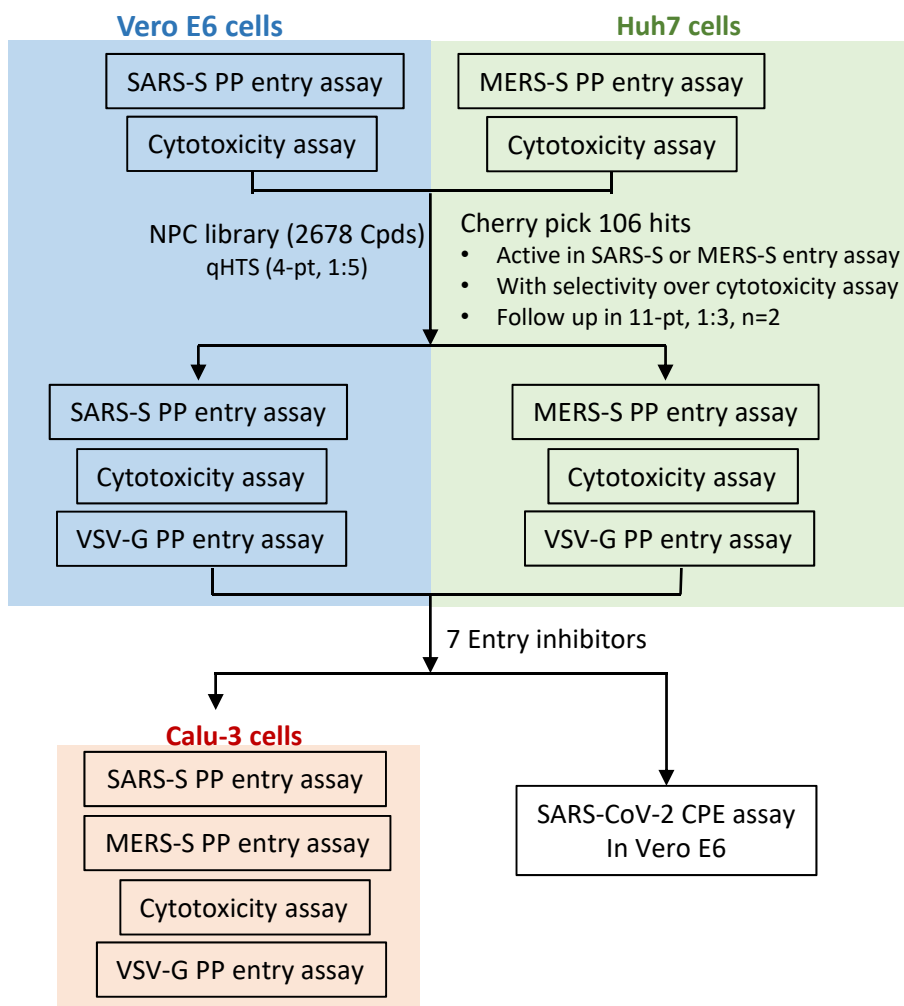
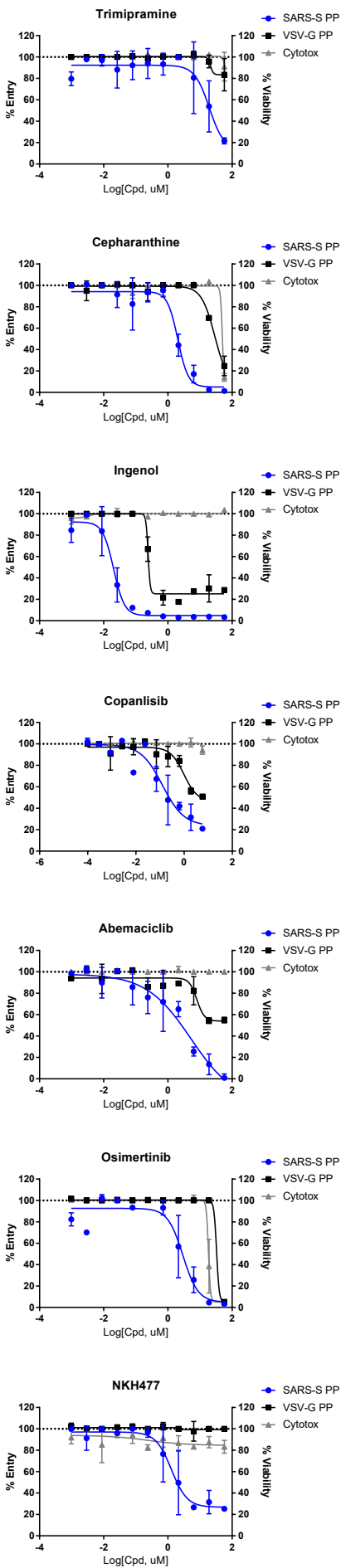


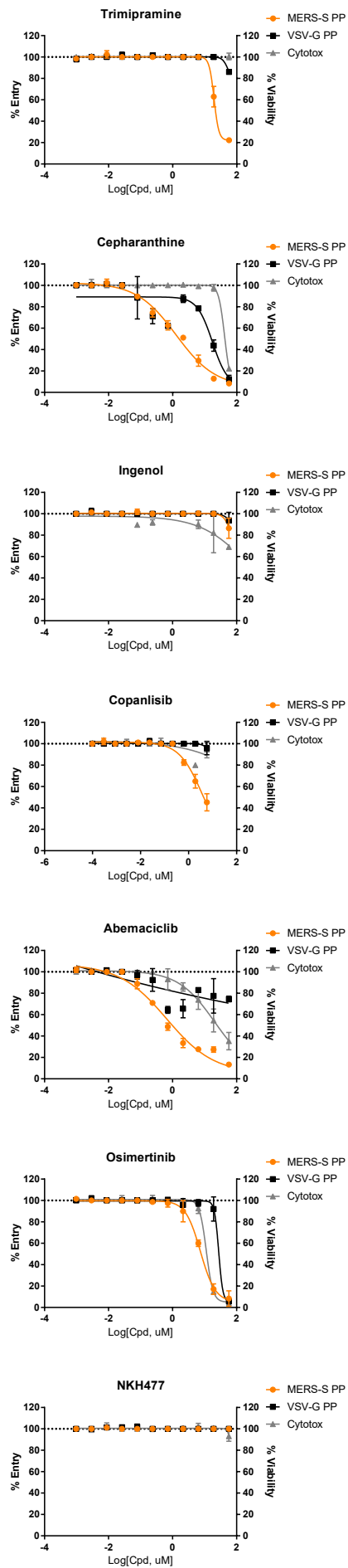
Figure 3.



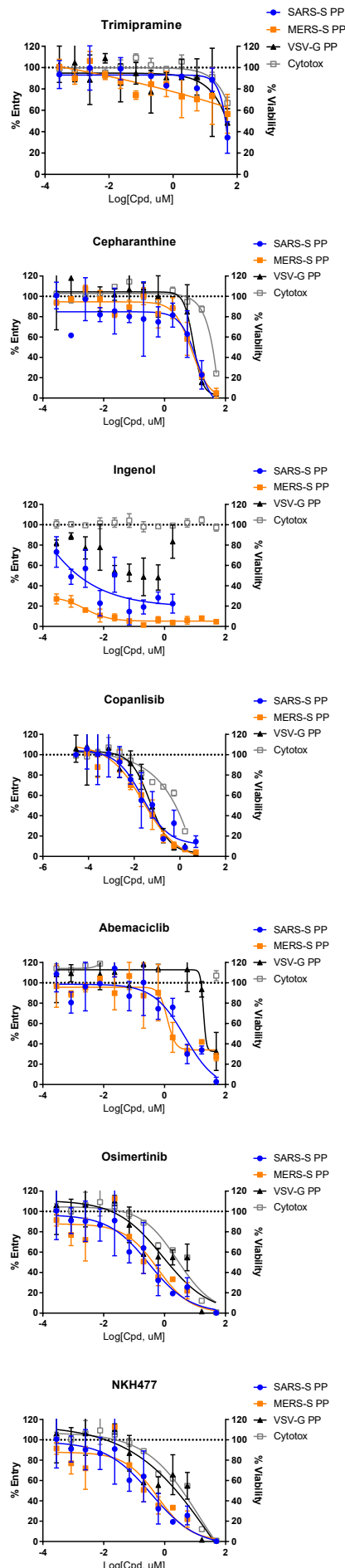
a. Vero E6 cells



b. Huh7 cells



c. Calu-3 cells



d. Structures

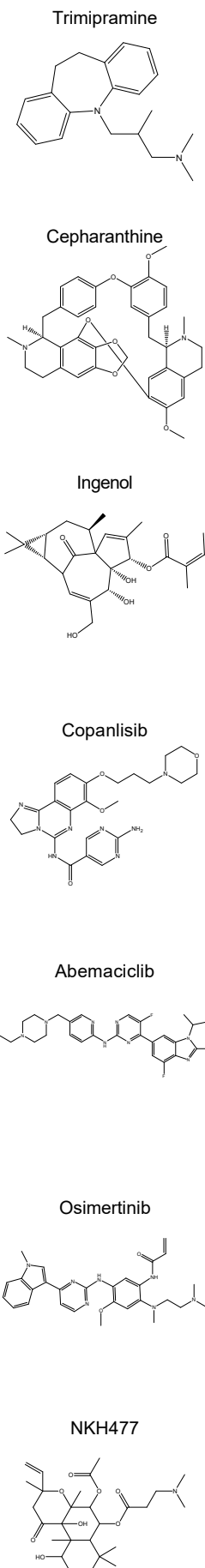


Figure 5

